Raman Laser Based on a Fiber with Variable Mode Structure

A. E. Bednyakova[a, *]**, M. P. Fedoruk**[b]**, A. S. Kurkov**[c]**,
E. M. Sholokhov**[c]**, and S. K. Turitsyn**[d]

[a] *Novosibirsk State University, ul. Pirogova 2, Novosibirsk, 630090 Russia*
[b] *Institute of Computational Technologies, pr. Akademika Lavrent'eva 6, Novosibirsk, 630090*
[c] *General Physics Institute, ul. Vavilova 38, Moscow, 119333 Russia*
[d] *School of Engineering and Applied Science, Aston University, Birmingham, B4 7ET United Kingdom*
*e-mail: anastasia.bednyakova@gmail.com
Received June 24, 2010; in final form, September 16, 2010

Abstract—A Raman converter based on an active fiber with variable mode structure is experimentally and theoretically studied. It is demonstrated that a conventional telecommunication fiber with variable mode structure can be used to construct Raman converters.

INTRODUCTION

Recent interest in fiber Raman lasers has been driven mainly by existing and possible applications [1]. Such devices allow the effective conversion of laser pump radiation into the radiation at lower frequencies (Stokes radiation) using the stimulated Raman scattering (SRS) in optical fiber. Note that a pump power of about 1 W is sufficient for the excitation of the stimulated Raman scattering in optical fibers.

Medium-power Raman converters serve as pump sources in erbium and SRS amplifiers of optical signals in several spectral ranges [2, 3]. They can also be employed in medicine, material processing, targeting systems, and wireless optical communications. Note that the diversified applications are possible due to the rare-earth doping in the SRS converters, which makes it possible to create fiber sources that emit at any wavelength in the spectral range 0.9–2.0 µm (almost the entire near-IR spectral range) [4–6]. The application of the fiber lasers with a radiation wavelength of about 2 µm [7, 8] allows the analysis of lasing in the mid-IR range. Note that the configuration of the Raman laser and the parameters of fiber that is used for the conver-

sion depend on the pump wavelength and the given emission wavelength of the converter.

One of the key problems in the construction of the Raman laser involves the selection of the active medium for the conversion. The fiber length in the converter can reach several hundred meters, and, hence, it is expedient to employ available telecommunication fibers (in particular, the SMF-28 fiber). Such a fiber is the two-mode fiber in the spectral range of the ytterbium laser and can be the single-mode fiber at the given wavelength of the output radiation. The purpose of this work is the construction and analysis of a two-stage SRS converter with an output radiation wavelength of about 1265 nm in which a conventional telecommunication fiber with variable mode structure serves as the active fiber. We choose the wavelength for pumping of SRS amplifiers and for medical applications [9].

EXPERIMENTAL SCHEME

Figure 1 demonstrates the laser scheme. Such a device allows the conversion of the pump radiation with a wavelength of 1123 nm into the Stokes radiation with a wavelength of 1265 nm.
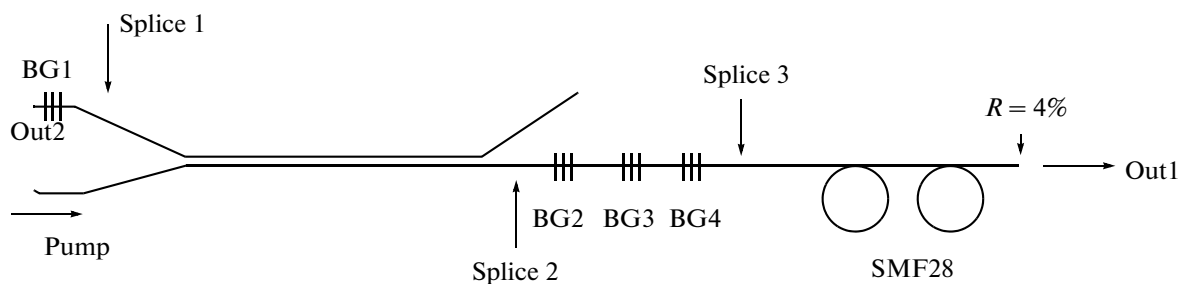

Fig. 1. Configuration of the two-stage Raman laser.

The SRS converter consists of an optical fiber and a set of Bragg gratings whose resonance wavelengths correspond to the Stokes shifts in the fiber material. The gratings were recorded using the interference method [10]. Note that the gratings tuned to the intermediate wavelengths normally have a reflection coefficient of about 100%. A distinctive feature of the above configuration is the absence of the Bragg gratings at the exit of the cavity. The feedback at a level of 4% is provided by the Fresnel reflection at the end surface of the fiber at all of the wavelengths. The absence of the output gratings allows a decrease in the uncertainty related to the loss caused by welding and gratings, makes it possible to eliminate the escape of radiation through Out 2 due to the spectral flowing, and allows an increase in the accuracy of numerical simulation.

Table 1 presents the reflection coefficients of the Bragg gratings.

An ytterbium laser with a maximum power of 9.22 W measured in front of Splice 3 serves as the pump source. It is expedient to employ the ytterbium-doped fiber laser owing to a relatively high efficiency in a wide spectral range.

A conventional SMF-28 fiber with a length of 1.09 km serves as the nonlinear medium of the laser. Such a fiber allows the propagation of two modes at a wavelength of 1123 nm and a single mode at a wavelength of 1265 nm.

The optical losses of the fiber at wavelengths of 1123, 1190, and 1265 nm are 0.8, 0.65, and 0.5 dB/km, respectively. We experimentally determine the gains. In addition, the calculations are performed with allowance for the intracavity loss related to the welding of the active fiber and the fiber with the recorded Bragg gratings and the additional scattering

Table 1

No.	Res. wavelength, nm	Reflection
BG1	1123	>99%
BG2	1123	25%
BG3	1190	>99%
BG4	1265	>99%

by the gratings. The total additional loss on Splice 3 is 1%.

The first and, then, second Stokes components emerge when the pump power increases. Figure 2 shows the output radiation spectrum at the maximum laser power. For all of the spectral components, we measure the dependence of the output power on the input power of the ytterbium laser (Fig. 3). Using the measured thresholds that correspond to the generation of the Stokes components, we can estimate the gains. The generation takes place when the two-pass gain is greater than the total intracavity loss. In the system under study, we consider the loss related to the escape of radiation through the free end surface (13.8 dB), the loss due to welding (0.1 dB for two passes), and the fiber loss at the length $2 \times 1090 = 2180$ m.

For the first conversion from 1123 to 1190 nm, the total loss is 15.7 dB. The threshold pump power is 2.9 W, and, for gain, we have $g = 15.7$ dB/(2.9 W $\times$ 2.18 km) = 2.5 dB/W km.

For the second conversion, the threshold power at a wavelength of 1190 nm is 3.95 W and the total loss is 15.1 dB. Then, we obtain $g = 15.1$ dB/(3.95 W $\times$ 2.18 km) = 1.75 dB/W km.
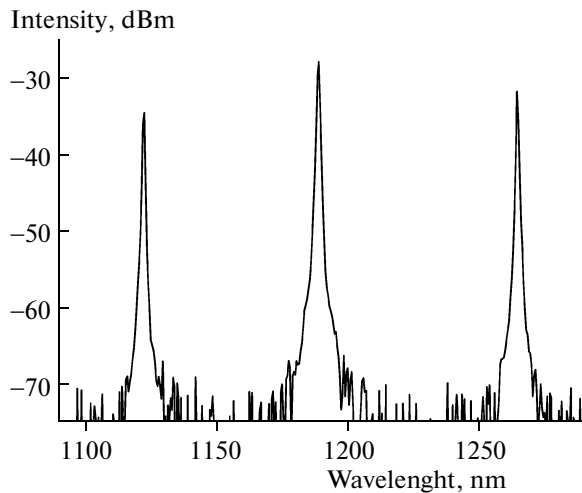
Fig. 2. Output radiation spectrum at the maximum laser power.
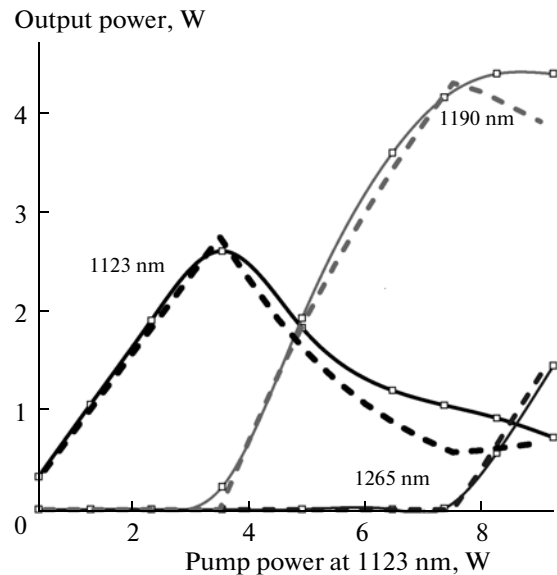
Fig. 3. Curves of (solid lines) experimental and (dashed lines) calculated output radiation powers.
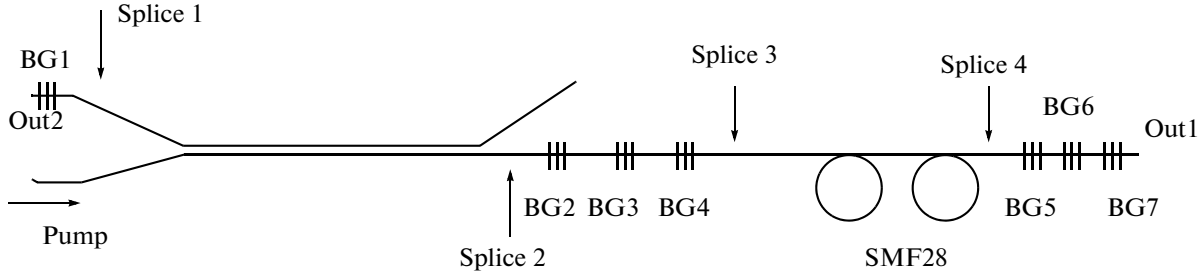
Fig. 4. Modified configuration of the two-stage Raman laser.

A relatively low gain for the first conversion can be due to an increase in the mode field diameter for the first and second modes. However, a sharp decrease in the gain on the second stage is related to the loss by the radiation of the second mode.

THEORETICAL MODEL

We simulate the two-stage converter using the numerical solution of the system of differential equations with the boundary conditions that describe the operation of the Raman laser in the quasi-monochromatic approximation [11, 12]. In the simulation, we assume that the fiber is single-mode at the pump wavelength. However, we perform the calculations with allowance for the loss related to the emission of the second mode. In addition, we neglect alternative nonlinear effects (in particular, the stimulated Mandelstam−Brillouin scattering). Such an approximation is valid for the pump fiber laser with a relatively wide radiation spectrum.

The system of equations for the evolution of the power of the pump waves that propagate in the forward and backward directions and for the Stokes radiation is represented as

$$\frac{dP_p^\pm}{dz} = \mp\alpha_p P_p^\pm \mp g_1 \frac{\nu_p}{\nu_1}(P_1^+ + P_1^-)P_p^\pm,$$

$$\frac{dP_1^\pm}{dz} = \mp\alpha_1 P_1^\pm \pm g_1(P_p^+ + P_p^-)P_1^\pm \mp g_2\frac{\nu_1}{\nu_2}(P_2^+ + P_2^-)P_1^\pm,$$

$$\frac{dP_2^\pm}{dz} = \mp\alpha_2 P_2^\pm \pm g_2(P_1^+ + P_1^-)P_2^\pm. \tag{1}$$

The boundary conditions ($N = 2$) are given by

$$P_p^+(0) = \beta_p^0 P_{in}, \quad P_p^-(L) = \beta_p^L R_p P_p^+(L),$$

$$P_i^+(0) = \beta_i^0 R_i P_i^-(0), \quad P_i^-(L) = \beta_i^L R_i P_i^+(L), \tag{2}$$

$$0 < i < N, \quad 0 < i < N,$$

$$P_N^+(0) = \beta_N^0 R_N P_N^-(0), \quad P_N^-(L) = \beta_N^L R_N P_N^+(L),$$

where z is the coordinate along the fiber; λ_p, λ_i, and λ_N are the wavelengths of pump radiation and Stokes components; and $P_p^\pm$, $P_i^\pm$, and $P_N^\pm$ are the powers of the pump and Stokes waves that propagate in the forward and backward directions along the z axis. The terms on the right-hand sides in system (1) that are linear with respect to power describe the optical loss in the fiber, and the nonlinear terms correspond to the SRS of the Stokes components or pump radiation. The fiber is characterized by optical loss α at the corresponding wavelength and gain g. The parameters of the cavity are taken into account in the boundary conditions at the entrance (2.1) and exit (2.2) of the cavity: L is the cavity length, R_i are the reflection coefficients of the corresponding Bragg gratings, and β is the quantity that characterizes the lumped loss in the cavity (loss due to welding and the nonresonant loss by Bragg gratings). We have $\beta = (100\% - p)/100\%$, where p is the fraction of radiation power in percents that is lost when the radiation passes through the splices and Bragg gratings.

We employ the collocation method to solve system of differential equations (1) with boundary conditions (2).

Table 2

Wavelength, nm	α, dB/km	G_R/A_{eff}, W m^{-1}
$\lambda_p = 1123$	0.8	2.5×10^{-3}
$\lambda_1 = 1190$	1.8	2.3×10^{-3}
$\lambda_2 = \lambda_{out} = 1265$	1.7	

Table 3

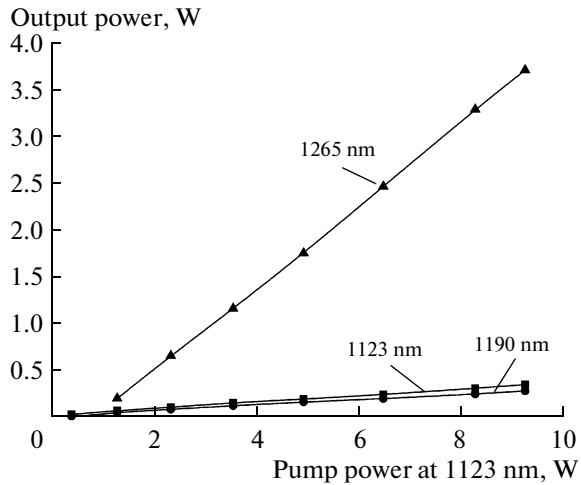| No.	Res. wavelength, nm	Reflection
BG5	1123	>99%
BG6	1190	>99%
BG7	1265	30%

Output power, W

Fig. 5. Plots of the output power of the Raman laser vs. the pump power.

RESULTS

Figure 3 demonstrates the experimental and calculated dependences of the intracavity pump power and the powers of Stokes components on the coordinate along the fiber in the Raman laser. It is seen that the numerical results are in good agreement with the experimental data for the laser configuration under study.

The maximum radiation power at $\lambda = 1265$ nm is 1.45 W when the pump power of the semiconductor laser is 9.22 W. The conversion efficiency of the fiber laser is 15%.

MODIFIED CONVERTER

We modify the configuration of the converter to reach the maximum power at a wavelength of 1265 nm (Fig. 4).

The fiber length in the cavity of the Raman laser is decreased to 300 m, and output Bragg gratings are added. Table 3 presents the parameters of the gratings.

Figure 5 shows the dependences of the output powers at the spectral components on the power of the ytterbium laser.

The maximum output power at a wavelength of 1265 nm is 3.7 W, and the corresponding conversion efficiency is 40%. Such an output power is sufficient for several applications. Note that the measured conversion efficiency can be greater than 50% when the converter is based on the fiber that works in the single mode regime for all of the spectral components [9].

CONCLUSIONS

We demonstrate that a conventional telecommunication fiber with variable mode structure can be used to construct SRS converters. The quasi-monochromatic theoretical model makes it possible to determine the main parameters of the SRS converter with a relatively high accuracy and allows a search for the optimal laser configurations. A transition from the two-mode regime to the single-mode regime of conversion leads to a decrease in the efficiency of the Raman laser.

REFERENCES

1. A. S. Kurkov and E. M. Dianov, Quantum Electron. **34**, 881 (2004).

2. A. S. Kurkov, V. M. Paramonov, O. N. Egorova, O. I. Medvedkov, E. M. Dianov, M. V. Yashkov, A. N. Gur'yanov, I. D. Zalevskii, and S. E. Goncharov, Quantum Electron. **31**, 801 (2001).

3. C. Headley and G. P. Agrawal, *Raman Amplification in Fiber Optical Communication Systems* (Academic, 2004).

4. A. S. Kurkov, E. M. Dianov, V. M. Paramonov, A. N. Gur'yanov, A. Yu. Laptev, V. F. Khopin, A. A. Umnikov, N. I. Vechkanov, O. I. Medvedkov, S. A. Vasil'ev, M. M. Bubnov, O. N. Egorova, S. L. Semenov, and E. V. Pershina, Quantum Electron. **30**, 791 (2000).

5. E. M. Dianov, A. S. Kurkov, O. I. Medvedkov, V. M. Paramonov, O. N. Egorova, N. Kurukitkoson, and S. K. Turitsyn, Laser Phys. **13**, 397 (2003).

6. E. M. Dianov, I. A. Bufetov, V. M. Mashinskii, A. V. Shubin, O. I. Medvedkov, A. E. Rakitin, M. A. Mel'kumov, V. F. Khopin, and A. N. Gur'yanov, Quantum Electron. **35**, 435 (2005).

7. A. S. Kurkov, E. M. Sholokhov, O. I. Medvedkov, V. V. Dvoyrin, Yu. N. Pyrkov, V. B. Tsvetkov, A. V. Marakulin, and L. A. Minashina, Laser Phys. Lett. **6**, 661 (2009).

8. A. S. Kurkov, E. M. Sholokhov, A. V. Marakulin, and L. A. Minashina, Laser Phys. Lett. **7**, 587 (2010).

9. A. S. Yusupov, S. E. Goncharov, I. D. Zalevskii, V. M. Paramonov, and A. S. Kurkov, Laser Physics, **20**, 357 (2010).

10. S. A. Vasil'ev, O. I. Medvedkov, I. G. Korolev, A. S. Bozhkov, A. S. Kurkov, and E. M. Dianov, Quantum Electron. **35**, 1085 (2005).

11. M. Rini, I. Cristiani, and V. Degiorgio, IEEE J. Quantum Electron. **36**, 1117 (2000).

12. W. A. Reed, W. C. Coughran, and S. G. Grubb, Technical Digest, OFC'95, WD1, 107 (1995).